Kinetics of XY and Ising ordering in a time-dependent Ginzburg-Landau model with $O(2)\times Z_2$ ground-state degeneracy

Sung Jong Lee,[1] Bongsoo Kim,[2] and Jong-Rim Lee[3]
[1]*Department of Physics, University of Suwon, Kyonggi-do 445-743, Korea*
[2]*Department of Physics, Changwon National University, Changwon 641-773, Korea*
[3]*NSSPC, College of Engineering, Changwon National University, Changwon 641-773, Korea*
(Received 28 February 1996; revised manuscript received 7 July 1997)

We investigate numerically the ordering dynamics of a time-dependent Ginzburg-Landau (TDGL) model in two dimensions, which possesses a ground-state manifold with $O(2)\times Z_2$ degeneracy. The ordering process of the system is described in terms of annihilation of both point defects (vortices) and line defects (domain walls), together with the mutual pinning between the two kinds of defects. There exist two regimes (regimes I and II) of parameter space with different growth kinetics. In regime I, Ising order shows a power law growth with exponent $\phi_I \simeq 0.48$, but XY order grows with smaller exponent of $\phi_{XY} \simeq 0.38$, while in regime II both Ising and XY order exhibit an effective growth exponent of $\phi_I \sim \phi_{XY} \simeq 0.38$. In regime II, the system exhibits a very slow approach to the asymptotic scaling regime. This distinction between the two regimes is attributed to the different nature of the symmetry of the Ising order parameter. [S1063-651X(97)07811-2]

PACS number(s): 64.60.Cn, 64.60.Ht, 64.60.My, 82.20.Mj

I. INTRODUCTION

There has been a long history of research activity on the phase ordering processes for statistical systems quenched from disordered phase to a low temperature ordered phase [1]. It is now fairly well established that the equal-time correlation functions at the late time stage exhibit scaling properties with typical size of the ordered regions growing as a power law in time, and that the growth law and the scaling functions depend on the dimensionality of the system, number of the order parameter components, and the conserved or nonconserved nature of the order parameter [2]. For systems with $O(N)$ symmetry, when the dimensionality of the system is not less than the number of components of the order parameter N, stable topological defect structures such as domain walls, vortices, strings, and monopoles are generated and the ordering dynamics of the system is known to be closely related to the decay process of these defects which act as disordering agents [3–7].

Most of the research in this area has focused on systems with a single kind of topological defect structure, and the phase ordering kinetics in systems in which two or more types of topological defects coexist and interact with each other was almost never explored. The two-dimensional Josephson junction array under a transverse magnetic field [8], discotic liquid crystals [9], and helimagnetic compounds [10] provide some physical examples of such systems.

Recently, the present authors [11] have performed numerical simulations on the ordering dynamics of the fully frustrated XY (FFXY) model on a square lattice [12] which possesses both continuous O(2) and discrete Z_2 degeneracies in its ground-state manifold. This model is known to describe the equilibrium properties of Josephson junction arrays in two dimensions with half magnetic flux quantum per unit plaquette [8]. This work indicated that the ordering dynamics of the model quenched from infinite temperature to a low temperature exhibits a rich variety of behaviors such as temperature-dependent ordering, a characteristic low temperature chiral domain morphology with faceted walls, and a finite temperature roughening transition separating the two different kinds of domain growth morphology [13].

In the present work, we investigate the ordering kinetics of a continuum time-dependent Ginzburg-Landau (TDGL) model, in two dimensions with $O(2)\times Z_2$ degeneracy, which is closely related to the FFXY model on a square lattice. The aim of the present work is to understand the effect of coexistence of both continuous and discrete broken symmetry (and interaction between the corresponding defect structures) on the ordering kinetics of the systems governed by the continuum TDGL models. The Ginzburg-Landau Hamiltonian can be derived from the FFXY model in two dimensions through a Hubbard-Stratonovich transformation as the effective free energy of the system at finite temperature [14]. It can also be constructed in terms of two planar vector fields by symmetry arguments [15]. It is shown below that, depending on the values of the coupling constants, there exist two characteristic regimes (regime I and regime II) with different growth kinetics. This is due to the existence of two types of Ising order parameters possible for the model. In regime I, the Ising order parameter can be identified as the inner product of the two planar vectors, while in regime II, the Ising order parameter corresponds to the difference between the squared amplitude of the two planar vector fields.

The main results of the present work are summarized as follows. The most important feature of the growth kinetics of the continuum TDGL model with $O(2)\times Z_2$ broken symmetry is that, for both regime I and regime II, the vortices are pinned near the Ising domain walls. This mutual pinning between vortices and domain walls is expected to influence the dynamic decay rate of the number of defects themselves, thus giving rise to nontrivial domain growth laws. Especially, the screening of vortex fields due to the domain walls appears to influence the equal-time correlation functions of the XY and Ising order parameters and their scaling func-

tions in an interesting way. In the case of regime I, Ising order grows with approximate domain length scale of $L_I \sim t^{\phi_I}$ with $\phi_I \simeq 0.48$ which is quite close to the domain growth in the scalar TDGL model with nonconserved order parameter. However, the length scale corresponding to XY order grows in time as a power law with $L_{XY}(t) \sim t^{\phi_{XY}}$, where $\phi_{XY} \simeq 0.38$, which is distinctly smaller than the pure XY growth exponent reported from various numerical simulations [16–19].

On the other hand, in the case of regime II, the Ising and XY order grow with nearly the same growth law of $L_{XY}(t) \sim L_I(t) \sim t^{0.38}$. This growth exponent, however, should be considered as only an effective growth exponent, because there exists a tendency of slow increase in the growth exponent with time. One interesting feature in regime II is that the Ising correlation function exhibits a very slow approach to the asymptotic limit. We attribute this to the high density of soft vortices pinned near the Ising domain walls. These vortices will be smearing the domain walls, making it difficult for the width of the domain walls to reach their equilibrium size. Hence, within our simulation time window, the effective Ising scaling function exhibits a singular behavior of $F(x) = 1 - Ax^{\chi}$ with $\chi \simeq 1.4$ near the origin, apparently violating Porod's law for the Ising order [2]. Time dependence of the vortex density and energy relaxation behavior are consistent with this picture of a broad Ising domain wall, very slowly approaching its equilibrium width as the ordering proceeds.

As for the autocorrelation function for the XY order parameter, for both regimes, it exhibits a stretched exponential behavior of $A_{XY}(t) \sim \exp(-ct^{\beta})$ with $\beta \simeq 0.2$. This peculiar behavior is reminiscent of the XY autocorrelation function in the one-dimensional (1D) O(2) model [20], though with different values of the β exponent [$\beta = 1/2$ in the 1D O(2) model].

This paper is organized as follows. In Sec. II we present the Hamiltonian of the model, the symmetry, the ground-state configurations, and the associated Langevin dynamic equation. Section III explains the results of numerical simulations. Section IV summarizes the main results of the present work.

II. TDGL MODELS WITH O(N)$\times Z_2$ GROUND-STATE DEGENERACY

We begin with a Ginzburg-Landau Hamiltonian based on two N-component real vectors $\vec{\phi}_1$ and $\vec{\phi}_2$ of the form

$$H = \int d^d r \left[\frac{1}{2} [(\vec{\nabla}\vec{\phi}_1)^2 + (\vec{\nabla}\vec{\phi}_2)^2] + \frac{1}{4}(\vec{\phi}_1^2 + \vec{\phi}_2^2 - 1)^2 + \frac{g}{2}(\vec{\phi}_1 \cdot \vec{\phi}_2)^2 + \frac{h}{2}\vec{\phi}_1^2 \vec{\phi}_2^2 \right]. \quad (1)$$

This Hamiltonian with $N = 2$ was derived by Choi and Doniach [14] through a Hubbard-Stratonovich transformation and by Yosefin and Domany [15] through a symmetry argument, in connection with efforts to understand the critical properties of the two-dimensional FFXY model. Let us first discuss the symmetry of the above Hamiltonian and the lowest energy configurations. In order to obtain the minimum energy configurations, it is enough to consider the spatially constant solution that satisfies the extremum condition for the potential term, i.e.,

$$\left. \frac{\delta V}{\delta \vec{\phi}_\alpha} \right|_{\vec{\phi} = \vec{\phi}_{\min}} = 0, \quad \alpha = 1,2 \quad (2)$$

where

$$V = \frac{1}{4}(\vec{\phi}_1^2 + \vec{\phi}_2^2 - 1)^2 + \frac{g}{2}(\vec{\phi}_1 \cdot \vec{\phi}_2)^2 + \frac{h}{2}\vec{\phi}_1^2 \vec{\phi}_2^2. \quad (3)$$

It can be shown from Eqs. (2) and (3) that there exist, in general, two different regimes in the (g,h) plane. These two regimes are characterized by different ground-state configurations and correspondingly by different definition of Ising order parameters. The underlying reason for the existence of two different Ising order parameters lies in the full symmetry structure of the Hamiltonian H. Namely, the Hamiltonian (1) is invariant under (i) a global (simultaneous) rotation of two vector fields [O(N)], (ii) the exchange of the two fields (Z_2^a), and (iii) the sign change (π rotation) of one of the fields (Z_2^b), where the superscripts a and b serve to distinguish the two discrete Z_2 symmetries. Hence the Hamiltonian has O(N)$\times Z_2^a \times Z_2^b$ symmetry. Among this full symmetry of the Hamiltonian, only O(N)$\times Z_2$ subsymmetry is broken in the ground state and depending on which one of the two Z_2 symmetries (Z_2^a or Z_2^b) is broken, two types of Ising order parameters are allowed. The two regimes are described in order.

Regime I: For $-2 < g + h < 0$ and $g < 0$, the ground-state configuration is obtained when the two fields $\vec{\phi}_1$ and $\vec{\phi}_2$ become parallel or antiparallel with the same amplitude $A = 1/\sqrt{g+h+2}$, which yields the ground-state energy $E_g = (g+h)/[4(g+h+2)]$. Therefore the proper Ising order parameter in this regime can be defined as

$$\chi(\vec{r},t) = [\vec{\phi}_1(\vec{r},t) \cdot \vec{\phi}_2(\vec{r},t)]/A^2. \quad (4)$$

Note that the two degenerate (parallel and antiparallel) ground-state manifolds can never be reached from each other by a global rotation of the two fields simultaneously. Within one vacuum manifold, a global rotation of an arbitrary angle of the two fields generates another ground-state configuration, representing O(N) degeneracy of the system. In addition, changing the sign of one of the two fields transforms one ground-state manifold into the other manifold with opposite Ising order parameter value. An arbitrary ground-state configuration is thus a symmetry broken state for both of these continuous and discrete symmetries, namely, O(N)$\times Z_2^b$ symmetry.

Regime II: For $g > 0$ and $h > 0$ the ground-state configurations are given by either one of the fields becoming a unit vector and the other field zero. That is, the relative amplitude of the two vectors determines the Ising order parameter of the model, which is defined as

$$\chi(\vec{r},t) = [\vec{\phi}_1(\vec{r},t)]^2 - [\vec{\phi}_2(\vec{r},t)]^2. \quad (5)$$

Again, in this regime, there exist two disconnected sets (by global rotations of the fields) of ground-state manifolds,

which is connected by exchange of the two fields $\vec{\phi}_1$ and $\vec{\phi}_2$ (Z_2^a). Therefore, as in regime I, the ground state possesses $O(N)\times Z_2^a$ degeneracies. But note that the nature of the discrete Z_2 symmetry for the two regimes is different: For regime I, this symmetry corresponds to changing the sign of one of the two fields whereas for regime II, it corresponds to exchange of two fields.

For the special case of $N=2$, which we will be focusing on in this work, in addition to the above two regimes, there appears an apparently new regime for $-2<h<0$ and $g>0$ where the two disconnected sets of ground-state configurations correspond to the perpendicular alignment of the two vector fields (clockwise or counterclockwise) with the same amplitude $A_c=1/\sqrt{h+2}$, thus forming positive and negative chirality ground-state manifolds, respectively. The chiral Ising order parameter is then defined as

$$\chi(\vec{r},t)=[\phi_{1x}(\vec{r},t)\phi_{2y}(\vec{r},t)-\phi_{1y}(\vec{r},t)\phi_{2x}(\vec{r},t)]/A_c^2, \quad (6)$$

where $\phi_{\alpha,i}$ denotes the ith component of the $\vec{\phi}_\alpha$ field. It should be emphasized that this regime is meaningful only for $N=2$ since for $N>2$ the above two chiral ground states are connected by a global rotation with respect to the line passing through the half angle between the two vector fields. However, one can easily verify that this regime is in fact equivalent to regime I by a simple linear transformation of the fields, i.e., by rotating one of the two fields by $\pi/2$.

We assume that the time evolution of the model is governed by the Langevin equation (model A dynamics [21]) corresponding to the nonconserved order parameter, of the form

$$\frac{\partial\vec{\phi}_\alpha}{\partial t}=-\frac{\delta H}{\delta\vec{\phi}_\alpha}, \quad \alpha=1,2 \quad (7)$$

where the thermal noise is ignored since we are concerned with only the zero temperature quench in the present work. Equation (7) is numerically integrated in time using the Euler method with the integration time step $\Delta t=0.1$ and the discrete lattice Laplacian with the mesh sizes $\Delta x=\Delta y=1$ is used in Eq. (7). Periodic boundary conditions in both lattice directions are employed. Simulations were carried out on square lattices of linear size $N=400$. The final results are obtained from averages over 20 to 30 different random initial configurations. Main quantities of interest are as follows.

(i) Equal-time correlation function for the XY order parameter

$$C_{XY}(r,t)=\frac{1}{2N^2}\left\langle\sum_{i,\alpha=1,2}\vec{\phi}_\alpha(i,t)\cdot\vec{\phi}_\alpha(i+r,t)\right\rangle. \quad (8)$$

(ii) Equal-time correlation function for the Ising order parameter

$$C_I(r,t)=\frac{1}{N^2}\left\langle\sum_i\chi(i,t)\chi(i+r,t)\right\rangle. \quad (9)$$

(iii) Autocorrelation function for the XY order parameter

$$A_{XY}(t)=\frac{1}{2N^2}\left\langle\sum_{i,\alpha=1,2}\vec{\phi}_\alpha(i,0)\cdot\vec{\phi}_\alpha(i,t)\right\rangle. \quad (10)$$

(iv) Autocorrelation function for the Ising order parameter

$$A_I(t)=\frac{1}{N^2}\left\langle\sum_i\chi(i,0)\chi(i,t)\right\rangle, \quad (11)$$

where $\langle\ \rangle$ denotes the average over random initial configurations. In addition to these quantities, we also measured the total number of vortices $N_V(t)$ corresponding to $\vec{\phi}_1$ and $\vec{\phi}_2$ at time t (which is defined as usual in terms of the phases of $\vec{\phi}_1$ and $\vec{\phi}_2$ respectively), and the excess energy relaxation $\Delta E(t)=\langle H\rangle-E_0$, E_0 being the ground-state energy.

III. SIMULATION RESULTS AND DISCUSSIONS

To begin with, it appears instructive to look into the domain growth morphology in terms of the distribution of point defects and Ising domain walls, which is shown in Fig. 1. We can clearly see that the vortices are pinned near Ising domain walls. This is intuitively appealing since near the domain walls the fields tend to change rapidly and due to this change the generation of vortices is more probable (less costly in energy) near the walls than anywhere else. In terms of domain growth, we therefore have an ordering system described by not a single length scale but multiple length scales such as Ising domain size and the average separation between vortices, etc., that can have, in general, different time dependence (i.e., power law exponents). Hence the question of dynamic scaling for our system with coupled order parameters takes on a more complicated form, since we can ask about the scaling properties of not only the correlation functions of each order parameter itself but also the cross-correlation functions between the two order parameters. From the viewpoint of structure of topological defects, this will turn into questions as to the density correlation of point defects, the density correlation of line defects, and also the cross-correlation between point defects and line defects [22–25]. Here, in this work, however, we focus for simplicity on the correlation functions of Ising order parameter and correlation functions of XY order parameter only.

A. Regime I

We tried to collapse the correlation functions for both XY and Ising order parameters in terms of the respective length scales $L_I(t)$ and $L_{XY}(t)$ which are defined as $C_I(r=L_I(t),t)=1/2$ and $C_{XY}(r=L_{XY}(t),t)=1/2$. We first discuss the scaling in the growth of XY order. As Figure 2 demonstrates, the XY correlation function satisfies a dynamic scaling of the form $C_{XY}(\vec{r},t)=F_{XY}(r/L_{XY}(t))$. The length scales $L_{XY}(t)$ shows a power law growth $L_{XY}(t)\sim t^{\phi_{XY}}$ with the growth exponent $\phi_{XY}\simeq 0.38$ for late time stage ($t\geqslant 80$), which is clearly smaller than the growth exponent in the pure XY model [16–19], as shown in Fig. 3. On the other hand, the time dependence of the length scale $L_I(t)$ (Fig. 3) extracted from the Ising correlation function shows initial slope (for $t\leqslant 80$) of $\phi_I\simeq 0.35$ and slowly approaches the value of $\phi_I(t)\simeq 0.48$, which is close to the curvature-driven exponent

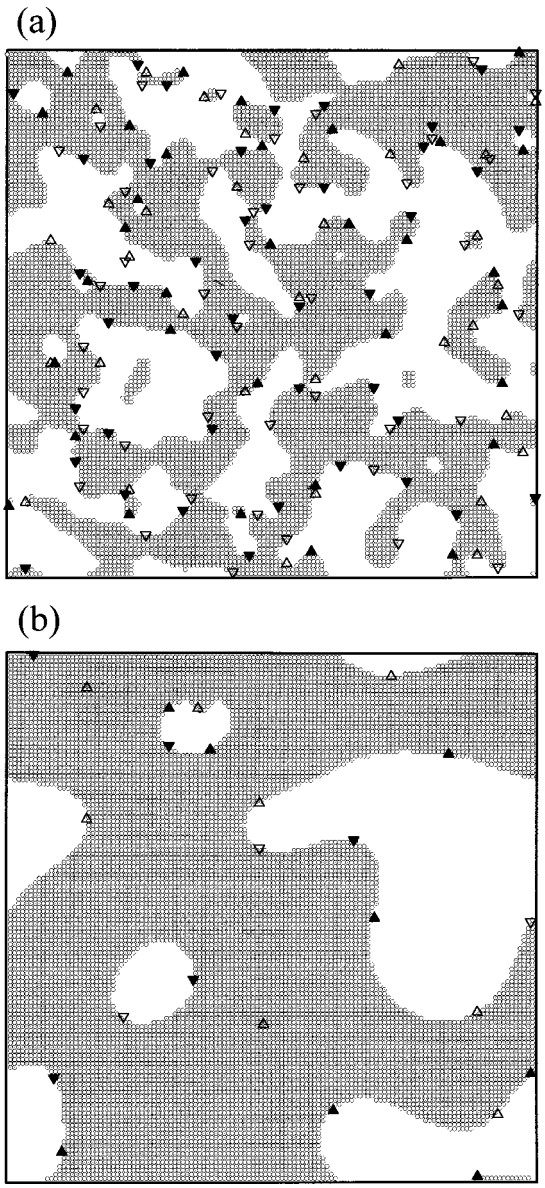

FIG. 1. Snapshots of configurations at various times for Ising domains and O(2) spin vortices in regime I: (a) $t=10$, (b) $t=160$. Shaded area represents Ising domains with positive sign (''spin up''). Triangles and inverse triangles represent the two kinds of vortices corresponding to ϕ_1 and ϕ_2 fields, respectively, with positive (filled) and negative (open) vorticities.

1/2. Evidently, two different length scales $L_I(t)$ and $L_{XY}(t)$ are involved in the ordering dynamics of the present model in regime I.

Now, we have to face the question as to the mechanism for these two different length scales, especially for the slower growth of XY order. One hint can be drawn from the morphological feature as mentioned above. That is, the domain walls interact with the point vortices and make them pinned near the walls. And this pinning impedes and slows down the motion of vortices, especially along the direction normal to the domain walls, which would result in a slower decay of the vortices. Since we expect the length scale $L_{XY}(t)$ is closely related to the average separation between vortices, we can understand at least qualitatively that $L_{XY}(t)$ grows with smaller power exponent than in the case of the pure XY

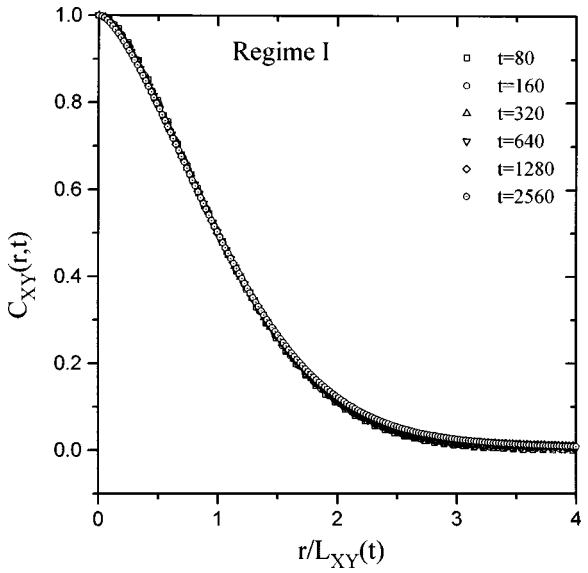

FIG. 2. Scaling collapse of the equal-time correlation functions for the XY order parameter in regime I.

model. Indeed, the time dependence of the vortex number, which is shown in Fig. 4, goes as $N_V(t)\sim t^{-0.76}$ at the late time stage, giving the average separation between vortices $L_V(t)\equiv 1/\sqrt{N_V(t)}\sim t^{0.38}$, which is comparable to the growth of the length scale $L_{XY}(t)$. Also, when we tried to collapse the XY correlation function with this length scale $L_V(t)$ directly extracted from the number of vortices $N_V(t)$, it yields a good scaling collapse (see Fig. 5). This seemingly plain result is actually an interesting feature that can be contrasted to the case of the pure XY model, where this method does not give a good scaling collapse due to different logarithmic corrections present in the two length scales $L_V(t)$ and $L_{XY}(t)$, as Blundell and Bray [17] explicitly demonstrated. Screening effect of Ising domain walls on the long range interaction between vortices may be the main cause behind

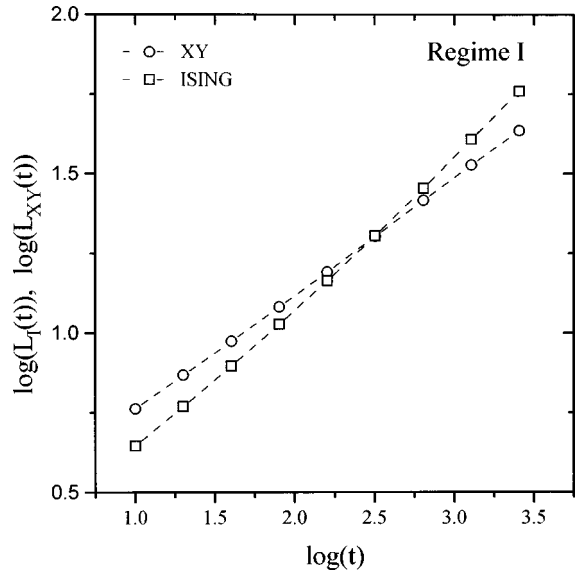

FIG. 3. Time dependence of the two length scales corresponding to XY and Ising order parameters in regime I. We obtain $L_{XY}(t)\sim t^{0.38}$ and $L_I(t)\sim t^{0.48}$ for late time region.

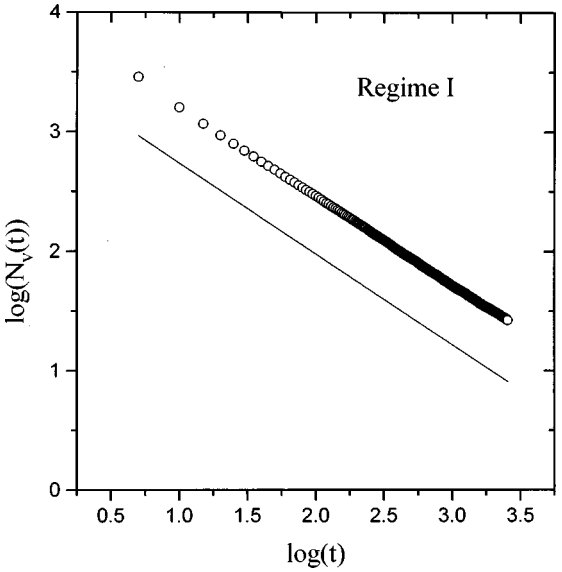

FIG. 4. Time dependence of the total number of vortices plus antivortices. The solid line represents a power law with slope -0.76.

this drastic reduction of the logarithmic correction in the growth of XY order.

Now we turn to the scaling function for the Ising order parameter. As can be seen in Fig. 6, the quality of the scaling collapse for the Ising order parameter is rather poor, or, to put it more precisely, the correlation functions in early time stages exhibit features with finite curvature near the origin, similar to the case of continuous vector order parameter and these correlation functions slowly approach the asymptotic scaling form. This can be attributed to the softness of domain walls from the continuum nature of the TDGL model; similar features can also be seen in the case of the usual scalar TDGL model.

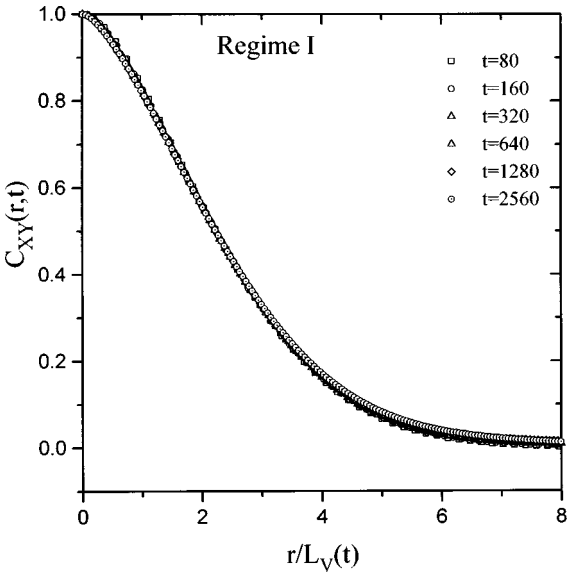

FIG. 5. Scaling collapse of the equal-time correlation functions for the XY order parameter in regime I with the length scale $L_V(t)$ extracted from the time dependence of the total number of vortices (Fig. 4). In contrast to the pure O(2) model, this yields a good scaling collapse.

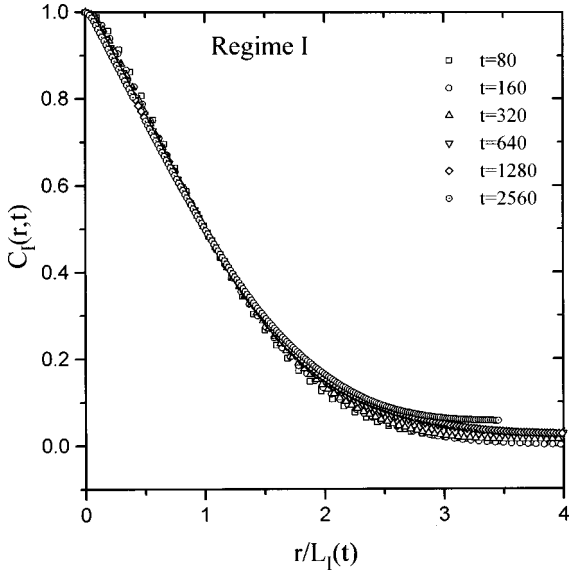

FIG. 6. Scaling collapse of the equal-time correlation functions for the Ising order parameter in regime I.

B. Regime II

Figure 7 shows the length scales $L_{XY}(t)$ and $L_I(t)$, from which we can extract an effective growth law of $L_{XY}(t) \sim L_I(t) \sim t^{0.38}$. Note also that from Fig. 8 the Ising correlation functions (similar to the case of regime I), show very slow approach to the asymptotic form. This can be contrasted with the XY correlation function which exhibits a relatively fast approach to its scaling limit, as shown in Fig. 9. In particular, we find that the asymptotic limit of the scaled correlation functions for the Ising order parameter does not show the usual short distance behavior of $F_I(x) \sim 1 - Ax$ but exhibits a finite curvature near the origin ($x = 0$) with resulting nontrivial Porod's law of $F_I(x) \sim 1 - Ax^{1.4}$. Unlike the case of regime I, this anomalous short distance behavior *does* persist over into the late time regime.

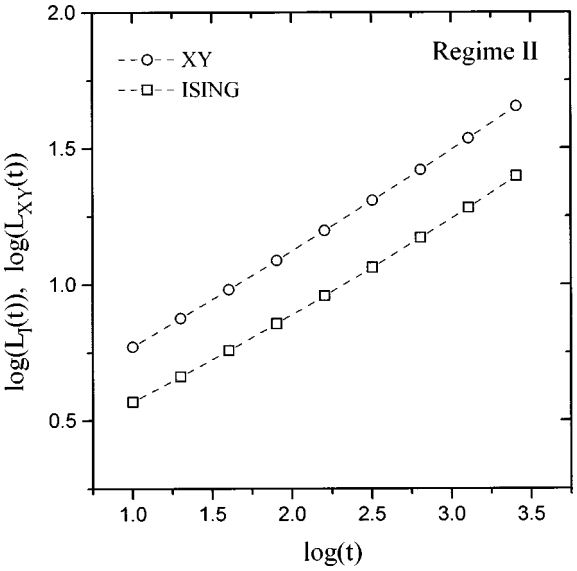

FIG. 7. Time dependence of the two length scales corresponding to XY and Ising order parameters in regime II. In contrast to regime I, they show a comparable growth rate $L_{XY}(t) \simeq L_I(t) \sim t^{0.38}$.

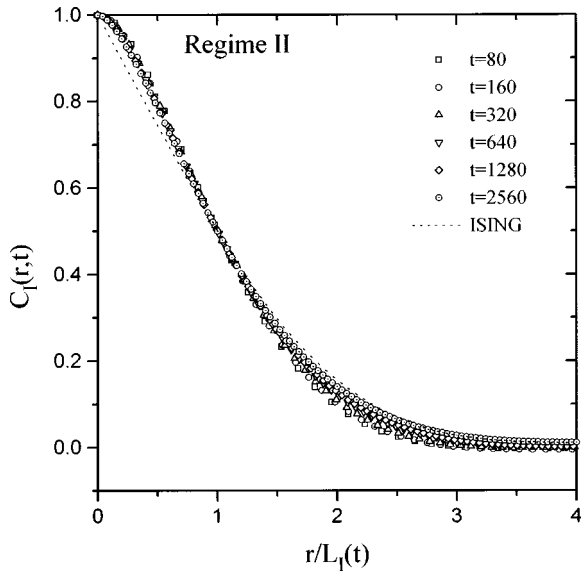

FIG. 8. Scaling collapse of the equal-time correlation functions for the Ising order parameter in regime II.

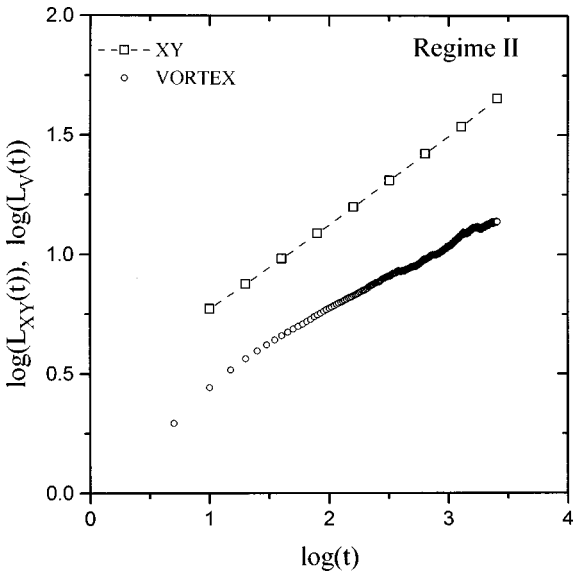

FIG. 10. Time dependence of the two length scales $L_{XY}(t)$ and $L_V(t)$ in regime II: they do not have the same power law growth, in contrast to the case of regime I.

As an effort to understand these features, we may note the crucial difference in the symmetry properties of the Ising order parameters in the two regimes. That is, in the case of regime I, the Ising order parameter (due to its inner product form) is invariant under the simultaneous global rotation of both vectors $\vec{\phi}_1$ and $\vec{\phi}_2$, while in the case of regime II, the Ising order parameter is invariant under a larger group including independent global rotations of either $\vec{\phi}_1$ or $\vec{\phi}_2$ as can be easily seen from the amplitude squared form of the definition of the Ising order parameter. Therefore, in the case of regime I, the fields $\vec{\phi}_1$ and $\vec{\phi}_2$ do not have to reduce their amplitudes $|\vec{\phi}_1|$ and $|\vec{\phi}_2|$ near domain walls. One of the two fields can simply be rotated by π across the domain wall, thereby making the Ising order parameter $\chi=\vec{\phi}_1\cdot\vec{\phi}_2$ vanish on the domain wall with $|\vec{\phi}_1|=|\vec{\phi}_2|=1$. In order for a point vortex to be pinned near a domain wall of this type, the vortex should be a ''hard'' vortex (vortex with small core size) with larger chemical potential.

In contrast, in the case of regime II, across a domain wall the order parameter changes from $\vec{\phi}_1^2=1$, $\vec{\phi}_2^2=0$ to $\vec{\phi}_1^2=0$, $\vec{\phi}_2^2=1$. That is, within the interfacial region, both of the amplitudes $\vec{\phi}_1^2$ and $\vec{\phi}_2^2$ should have values much smaller than 1, the equilibrium value. Therefore we can have many ''soft'' vortices (vortices with large core size) with relatively smaller chemical potential near the domain wall region due to smaller amplitude values of the two fields near the interface region. It appears to be difficult to formulate an analytic argument for the effect of the pinning of the proliferating soft vortices on the domain wall dynamics. But, we can expect that these many soft vortices pinned near the domain wall region would smear out the domain wall profiles, slowing down the growth of Ising domains. We can partly check this expectation by measuring the number density of vortices $N_V(t)$ or the length scale $L_V(t)\sim 1/\sqrt{N_V(t)}$. As shown in Fig. 10, $L_V(t)\sim t^{0.29}$, while $L_{XY}(t)\sim t^{0.38}$. This means that many soft vortices are pinned near the domain walls and these vortices do not decay away as quickly as in the case of regime I. This, in turn, implies that the width of Ising domain walls would be very slow in approaching its equilibrium value. The above argument, at least, gives us a qualitative understanding as to why the Ising length scale $L_I(t)$ grows so slowly and why the scaled correlation function approaches a seemingly non-Ising scaling form with an anomalous effective Porod law exponent.

In the absence of a microscopic theory for the growth laws, we tried to find some relationships between various exponents, that can be checked from the simulation results. One relation we can start with is Porod's law and the exponents for the excess energy relaxation. As shown by Bray and Rutenberg [26], Porod's law, i.e., the short distance behavior of the scaling function, determines the long-time behavior of the excess energy relaxation, which is shown in Fig. 11. Now, assuming the dominance of the Ising length scale, Bray argument gives $\Delta E(t)\sim L_I(t)^{-\psi}$, where ψ is the

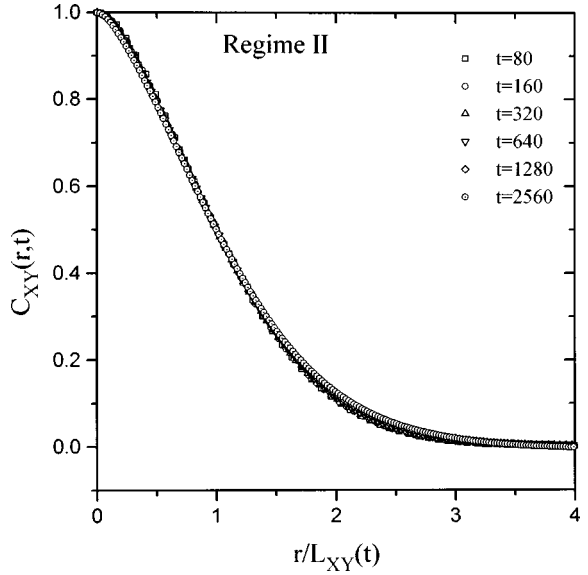

FIG. 9. Scaling collapse of the equal-time correlation functions for the *XY* order parameter in regime II.

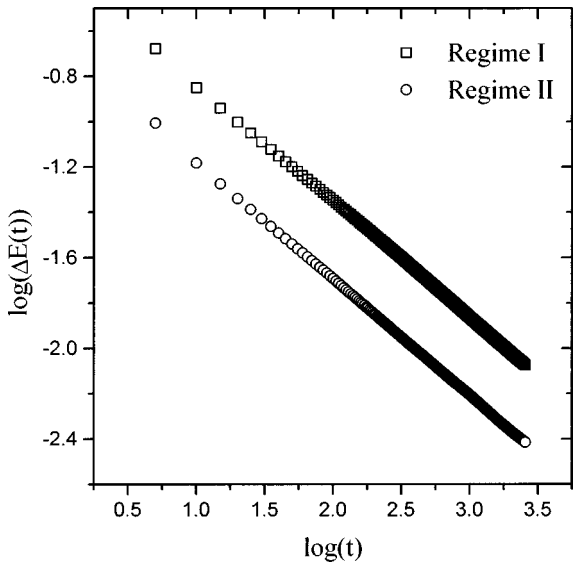

FIG. 11. Relaxation of the excess energy for regimes I and II. In both regimes, they show a power law decay $\Delta E(t) \sim t^{-\gamma}$ with $\gamma \simeq 0.52$.

exponent appearing in the short distance behavior of the scaling function of Ising order parameter. If we set the energy relaxation in time as $\Delta E \sim t^{-\gamma}$, then we see that $\Delta E(t) \sim t^{-\gamma} \sim L_I(t)^{-\gamma/\phi_I}$ where ϕ_I is the Ising growth exponent. Therefore we get the relation $\gamma = \psi \phi_I$, which can be checked using simulation results. First consider the case of regime I where we have $\gamma \simeq 0.52$, $\phi_I \simeq 0.48$, and $\psi \approx 1.1$, which closely satisfies the above relation. Next, in the case of regime II, we have $\gamma \simeq 0.52$, $\phi_I \simeq 0.38$, and $\psi \approx 1.4$, which, again, are seen to be consistent with the above scaling relation.

Lastly, we present the behavior of autocorrelation functions for the Ising and XY order parameters. As Fig. 12 demonstrates, the XY autocorrelation exhibits a stretched exponential behavior $A_{XY}(t) \sim \exp(-ct^{\beta})$ with the values of $\beta \simeq 0.20$ for both regimes. As seen in Fig. 1, the snapshots of growth morphology, the vortices are rarely located well inside Ising domains due to their pinning near the Ising walls and hence the dominant disorder within an Ising domain is the spin wave excitation. Therefore we can conjecture that the long-time behavior of the autocorrelation function for the XY order parameter is governed by these spin wave excitations, which will give rise to a stretched exponential behavior, just as in the case of the XY model in one dimension. It is worth mentioning that the recent numerical simulations carried out by Lee *et al.* [27] on the phase ordering in a coupled XY-Ising model [15,28] also show a similar stretched exponential relaxation for the XY autocorrelation function. Ising order parameter autocorrelation shows a power law relaxation with $A_I(t) \sim t^{-\lambda}$ with $\lambda \approx 0.6$, as shown in Fig. 13. But the statistics of the data is not good enough to determine whether the power law exponent is the same as the known exact value for the pure Ising case $\lambda = 5/8$ [29] or not.

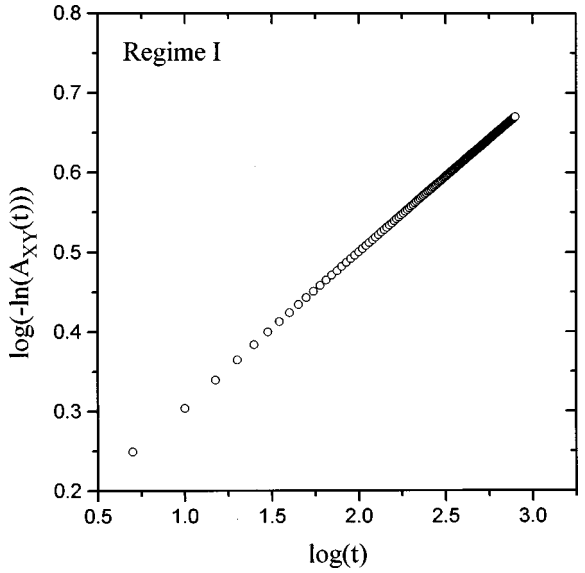

FIG. 12. Relaxation of the autocorrelation function for the XY order parameter: it can be well fitted by a stretched exponential relaxation of the form $A_{XY}(t) \sim \exp(-ct^{\beta})$ with $\beta \simeq 0.20$.

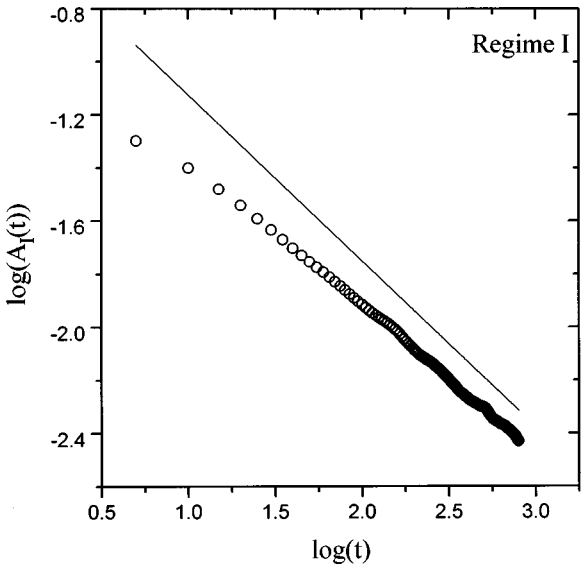

FIG. 13. The autocorrelation function for the Ising order parameter. We can see that the statistics is not as good as in the case of spin autocorrelation function (Fig. 12). The solid line represents a power law with slope $-5/8$.

To summarize the above results on the phase ordering of the TDGL model with $O(2) \times Z_2$ degeneracy in regimes I and II, we can compare these results with those of related model systems possessing the same ground-state degeneracy. We first note that even though the present TDGL model was derived from the FFXY model as an effective free energy at a finite temperature, the growth law features and morphologies of the domain growth in the present TDGL model do not show any similarity to those of the FFXY model. Rather, another variant system, which is called a coupled XY-Ising model [15,28], at finite temperature exhibits ordering kinetics quite close to the present TDGL systems in regime I [27]. In particular, for a wide range of intermediate temperatures, the growth exponent for XY order in this coupled XY-Ising model becomes $\phi_{XY} \simeq 0.36 \sim 0.39$, while the growth exponent for the Ising order shows $\phi_I \simeq 0.45 - 0.5$, which are close to those exponents of the TDGL model in regime I. One caveat, however, is that in the case of the coupled XY-Ising model at finite temperature, the XY ordering is the time

evolution toward a quasi-long-range order, where a critical dynamic scaling (rather than simple dynamic scaling) is satisfied for the XY correlation function. As shown above, the stretched exponential behavior of the XY autocorrelation function in the present TDGL model is also appearing in the coupled XY Ising model in contrast to the case of the FF XY model in two dimensions.

This may be understood in terms of the characteristics of point defects in each of those model systems. That is, in the case of the FFXY model, point defects are inevitably associated with corners of Ising (chirality) domain walls and these corner vortices interact with one another logarithmically. On the other hand, in the case of the coupled XY-Ising model or the present continuum TDGL model, point vortices do not have to reside on the corners of the Ising domain walls, even though it is relatively easier for the point vortices to be pinned on the corners of Ising domain walls. As for the TDGL model in regime II, we have not been able to find a related model system with analogous ordering characteristics.

IV. SUMMARY

In this work we presented simulation results on the ordering dynamics of the $O(2)\times Z_2$ TDGL model in two dimensions. We find that there exist two regimes of the model with distinct growth kinetics where, in regime I, the XY order exhibits a slower growth than that of the Ising order, while on the other hand, in the case of regime II, the two order parameters grow with length scales of the same effective growth exponent. Different symmetry nature of the Ising order parameter in the two regimes seems to cause distinct properties of mutual pinning between the vortices and domain walls, which in turn is expected to give rise to nontrivial growth characteristics. Unusual stretched exponential behavior is observed throughout the parameter space (both regime I and regime II) for the XY autocorrelation function, while a power law behavior is shown by Ising autocorrelation functions. In this work we considered only the self-correlation functions of Ising and XY order parameters. But it is expected that the mutual correlation function (appropriately defined) would give further information about the scaling properties of the growth kinetics of the model system with mixed ground-state degeneracies. Analytic treatment of the system (e.g., using Gaussian auxiliary field methods [3–5]) would be very welcome.

ACKNOWLEDGMENTS

We thank M. Y. Choi, Seunghwan Kim, and J. C. Lee for valuable discussions. This work was supported in part by the Basic Science Research Institute Program, Ministry of Education, Project No. BSRI-97-2412, the Korea Research Foundation under Grant No. 1997-003-D00086 (S.J.L.), and by the KOSEF (J.-R.L.).

[1] J. D. Gunton, M. San Miguel, and P. S. Sahni, in *Phase Transitions and Critical Phenomena*, edited by C. Domb and J. L. Lebowitz (Academic, New York, 1983), Vol. 8; H. Furukawa, Adv. Phys. **34**, 703 (1985); K. Binder, Rep. Prog. Theor. Phys. **50**, 783 (1987).
[2] A. J. Bray, Adv. Phys. **43**, 357 (1994).
[3] A. J. Bray and S. Puri, Phys. Rev. Lett. **67**, 2670 (1991).
[4] F. Liu and G. F. Mazenko, Phys. Rev. B **45**, 6989 (1992), and references therein.
[5] H. Toyoki, Phys. Rev. B **45**, 1965 (1992).
[6] A. J. Bray, in *Phase Transitions and Relaxation in Systems with Competing Energy Scales*, edited by T. Riste and D. Sherrington (Kluwer Academic, Boston, 1993).
[7] See the articles in *Formation and Interaction of Topological Defects*, edited by A.-C. Davis and R. Brandenberger (Plenum, New York, 1995).
[8] S. Teitel and C. Jayaprakash, Phys. Rev. Lett. **51**, 199 (1983); Phys. Rev. B **27**, 598 (1983); G. Ramirez-Santiago and J. V. José, *ibid.* **49**, 9567 (1994), and references therein.
[9] M. Hébert and A. Caillé, Phys. Rev. E **51**, R1651 (1995).
[10] G. Uimin and A. Pimpinelli, Phys. Rev. E **49**, 1123 (1994).
[11] S. J. Lee, J.-R. Lee, and B. Kim, Phys. Rev. E **51**, R4 (1995).
[12] J. Villain, J. Phys. C **10**, 4793 (1977); J. Phys. (Paris) **38**, 26 (1977).
[13] J.-R. Lee, S. J. Lee, B. Kim, and I. Chang, Phys. Rev. Lett. **79**, 2172 (1997).
[14] M. Y. Choi and S. Doniach, Phys. Rev. B **31**, 4516 (1985).
[15] M. Yosefin and E. Domany, Phys. Rev. B **32**, 1778 (1985).
[16] B. Yurke, A. N. Pargellis, T. Kovacs, and D. A. Huse, Phys. Rev. E **47**, 1525 (1993).
[17] R. E. Blundell and A. J. Bray, Phys. Rev. E **49**, 4925 (1994).
[18] M. Zapotocky, P. M. Goldbart, and N. Goldenfeld, Phys. Rev. E **51**, 1216 (1995).
[19] J.-R. Lee, S. J. Lee, and B. Kim, Phys. Rev. E **52**, 1550 (1995).
[20] T. J. Newman, A. J. Bray, and M. A. Moore, Phys. Rev. B **42**, 4514 (1990).
[21] P. C. Hohenberg and B. I. Halperin, Rev. Mod. Phys. **49**, 435 (1977).
[22] B. I. Halperin, in *Physics of Defects*, edited by R. Balian *et al.* (North-Holland, Amsterdam, 1981).
[23] M. Mondello and N. Goldenfeld, Phys. Rev. A **42**, 5865 (1990).
[24] F. Liu and G. F. Mazenko, Phys. Rev. B **46**, 5963 (1992).
[25] G. F. Mazenko and R. A. Wickam, Phys. Rev. E **55**, 1321 (1997); **55**, 5113 (1997); e-print cond-mat/9704250.
[26] A. J. Bray and A. D. Rutenberg, Phys. Rev. E **49**, R27 (1994); A. D. Rutenberg and A. J. Bray, *ibid.* **51**, 5499 (1995).
[27] J.-R. Lee, S. J. Lee, B. Kim, and I. Chang, Phys. Rev. E **54**, 3257 (1996).
[28] J. Lee, E. Granato, and J. M. Kosteritz, Phys. Rev. B **44**, 4819 (1991).
[29] D. S. Fisher and D. A. Huse, Phys. Rev. B **38**, 373 (1988).